Crystallization Kinetics of Glyme−LiX and PEO−LiX Polymer Electrolytes

Wesley A. Henderson†

Department of Chemical Engineering & Materials Science, University of Minnesota, Minneapolis, Minnesota 55455

Received August 14, 2006; Revised Manuscript Received May 16, 2007

ABSTRACT: The crystallization kinetics of oligomeric polyethers (glymes) and poly(ethylene oxide) (PEO) with a wide range of lithium salts including LiBETI, LiTFSI, $LiAsF_6$, $LiPF_6$, $LiClO_4$, LiI, $LiBF_4$, $LiCF_3SO_3$, $LiNO_3$, and $LiCF_3CO_2$ have been examined in detail. Wide variations exist between the rates of crystallization of the phases. These variations are strongly dependent upon the lithium salt present and are well correlated with the ionic association behavior of the different lithium salts in aprotic solvents.

1. Introduction

Glymes are short methyl-capped ethylene oxide oligomers, $CH_3OCH_2-(CH_2OCH_2)_n-H$ ($n = 1-4$ for monoglyme−tetraglyme or G1−G4, respectively) which resemble poly(ethylene oxide) (PEO). As such, glymes are excellent model compounds for studying the molecular interactions of PEO with ions. Over the course of the study of the crystalline phase behavior of lithium salts (LiX) with glymes[1] and PEO, it became clear that the phase behavior and crystallization kinetics of solvate phases were directly linked to the degree of ionic association in solution or the melt. Numerous reports have noted the widely varying crystallization kinetics observed in PEO−LiX electrolytes with different salts,[2−19] but explanations for these observations have been slow in coming. An understanding of how salt properties, salt concentration, and other factors such as temperature influence crystallization kinetics is critical to optimizing these materials for electrolyte applications. For example, Figure 1 shows the strong link between ionic conductivity and electrolyte crystallinity for $P(EO)_n$−LiTFSI ($LiN(SO_2CF_3)_2$) mixtures with $n = 6$, 10, and 14. Since crystallization is a transition between two physical states, the process is governed by the molecular interactions of the polyether−LiX mixtures in both the crystalline solid and liquid (or amorphous solid) melt. Unfortunately, the structural properties of the melt state remain poorly understood. It is hoped that the present discussion will add to the understanding of how solid crystalline solvate phase behavior and the properties of ions in liquid or amorphous polyether solvent mixtures are strongly linked together.

2. Experimental Section

Sample preparation and handling occurred in a dry room environment (<1% relative humidity, 22 °C). Glyme−LiX mixtures were prepared as indicated previously.[1] PEO−LiX mixtures were prepared with either low molecular weight PEO(2000)−poly(ethylene glycol) dimethyl ether or PEGDME (average M_n ca. 2000) (Aldrich) or high molecular weight PEO (average M_n ca. 5×10^6) (Aldrich). PEO electrolytes were prepared by stirring the salts and PEO in anhydrous acetonitrile overnight to form homogeneous solutions. In most cases, the solutions were clear; however, those containing $LiBF_4$ remained cloudy. The solutions were poured into Teflon dishes in a dry room fume hood and allowed to dry overnight. The materials were subsequently dried under vacuum at 65−80 °C for 24 h (except for the $LiAsF_6$ and $LiPF_6$ electrolytes as these were not thermally stable at this temperature for this period of time—these were dried at room temperature under vacuum for 48 h). In many cases, further annealing was necessary for the various samples to form homogeneous phases for XRD analysis.

DSC heating and cooling traces were obtained using a liquid nitrogen cooled Perkin-Elmer Pyris 1 differential scanning calorimeter. Small amounts of the samples (8−25 mg) were hermetically sealed in Al pans. For the glyme mixtures, it was often necessary to heat the mixtures while stirring to form homogeneous solutions for this purpose. Some of the sample pans were stored in a freezer in hermetically sealed coffee bags prior to analysis. In some cases, the samples were "annealed" by thermally cycling them at lower temperatures. The background has been subtracted from the DSC traces shown. Reported melting temperatures (mp's) are the endothermic peak temperatures. Wide-angle X-ray (WAX) powder diffraction analysis was performed on a Bruker-AXS microdiffractometer with a 2.2 kW sealed Cu X-ray Source. Samples were sealed in glass capillary tubes in the dry room before analysis.

3. Results and Discussion

Ionic Association. It is important to emphasize the relative degree of ionic association of various LiX salts in ether solvents. This may be obtained from an examination of the reported ionic association constants/vibrational spectroscopic bands of different salts in aprotic solvent−LiX mixtures. The order of increasing ionic association is found to be[1]

$$LiBPh_4 < LiBETI, LiTFSI, LiSbF_6, LiAsF_6 < LiPF_6 < LiClO_4, LiI < LiBF_4 < LiCF_3SO_3 < LiBr < LiNO_3 < LiCF_3CO_2$$

where LiTFSI and LiBETI denote $LiN(SO_2CF_3)_2$ and $LiN(SO_2C_2F_5)_2$, respectively.

Further information can be found by a comparison of which glyme−LiX solvates form and their thermal stability. Different forms of solvate structures may exist in either the crystalline or liquid phases. These include solvent-separated ion pair (SSIP), contact ion pair (CIP), or aggregate (AGG) solvates in which the ions are coordinated to zero, one, or more than one counterion, respectively. Crystalline SSIPs only form when the Li^+ cations and anions are highly dissociated, i.e., when the Li^+ cations are highly solvated by 4−6 (and in a few instances up to 8) ether oxygens (EOs). Typically, ionic association

† Current address: Department of Chemical & Biomolecular Engineering, North Carolina State University, 911 Partners Way, PO Box 7905, Raleigh, NC 27695-7905.

10.1021/ma061866d CCC: $37.00
Published on Web 06/15/2007

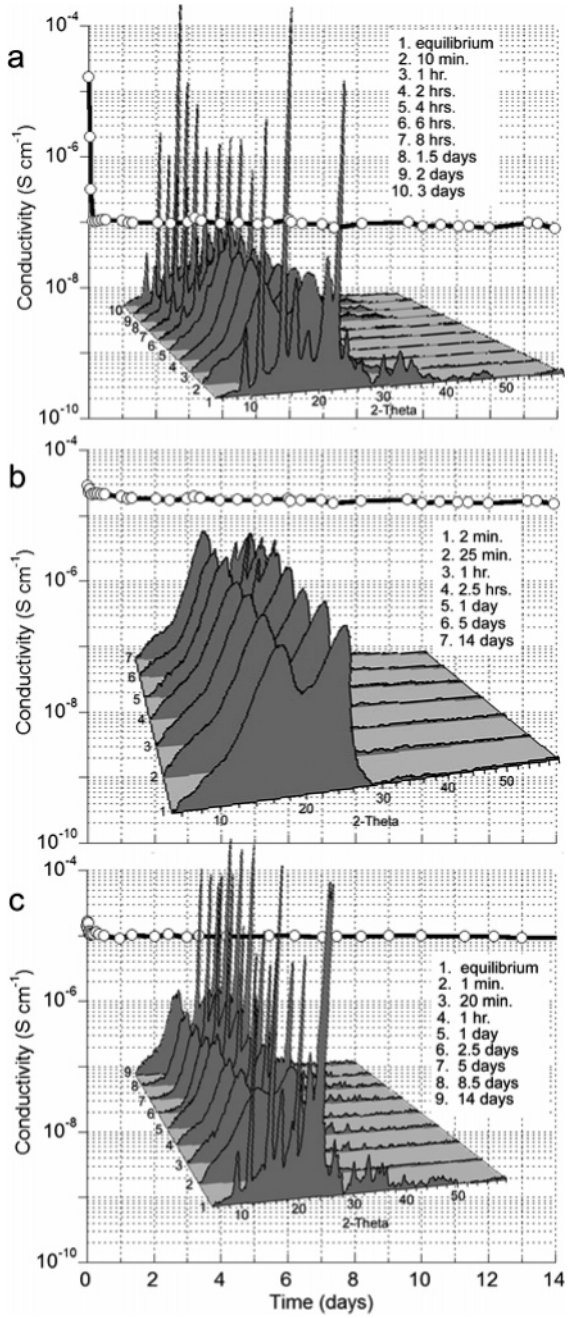

Figure 1. Isothermal ionic conductivity (25 °C) after quenching from the melt of $P(EO)_n(5 \times 10^6)$−LiTFSI electrolytes: (a) EO/Li = 6, (b) EO/Li = 10, and (c) EO/Li = 14. Powder XRD plots at 25 °C shown for different times after quenching from the melt at 100 °C (equilibrium indicates the initial fully crystalline electrolyte).

increases with increasing temperature and increasing salt concentration. Melting of the crystalline solvates may correspond to a disordering of the structure in which the general forms of Li^+ cation coordination and ionic association remain largely unchanged. Alternatively, melting may occur when the thermal energy destabilizes the existing structure to the extent where the Li^+ cation coordination changes. This may involve the replacement of coordinating solvent donor atoms with one or more anions leading to higher ionic association. Many factors will govern the melting process. The influence of the ionic association strength will be prominent when other factors (i.e., solvate crystal packing, size and shape of anions, etc.) are of similar magnitude. Examples are noted below.

In G1/LiX mixtures, the mp's of the CIP 2/1 solvates increase in the order

$$LiCF_3SO_3\ (4\ °C) < LiBF_4\ (34\ °C) < LiClO_4\ (64\ °C) < LiI\ (73\ °C)$$

The crystal structures of the $(G1)_2$:LiX solvates with LiBr,[20−22] LiSCN,[20] $LiBF_4$,[23] $LiClO_4$,[24] and LiI[25] are known. All have the same general structure with each Li^+ cation coordinated by two G1 molecules with four EOs and a single anion. Vibrational spectroscopy has indicated that when the CIP $(G1)_2$:$LiCF_3SO_3$ solvate melts, a large fraction of the solvated Li^+ cations become AGGs.[20,26] This suggests that a second anion replaces one of the G1 molecules coordinating the Li^+ cations. The ordering of the solvate mp's should therefore reflect the ionic association tendency of the salts with the most associated salt having the lowest solvate mp (i.e., the greatest tendency for solvent replacement by an anion). Note that LiBr does not follow this trend since the 2/1 solvate (42 °C) has a mp slightly higher than with $LiBF_4$. The reason for this is unknown, but it may be due to the differences in anion size and the corresponding steric effects.

In G2/LiX mixtures, SSIP 2/1 crystalline solvates form for all of the salts studied except $LiCF_3CO_2$.[1] Once again, the mp's mirror the ionic association ordering:

$$LiNO_3\ (-38\ °C) < LiBr\ (-11\ °C) < LiCF_3SO_3\ (-6\ °C) < LiBF_4\ (29\ °C) < LiClO_4\ (71\ °C) < LiI\ (81\ °C) < LiAsF_6\ (156\ °C)$$

The crystal structures of the $(G2)_2$:LiX solvates with $LiBF_4$,[27] $LiClO_4$,[24] $LiSbF_6$,[28] and LiTFSI[29] are known. All have the same general structure with each Li^+ cation coordinated by two G2 molecules with six EOs. The anions are uncoordinated. The lower mp's for the 2/1 solvates with LiTFSI (72 °C) and LiBETI (92 °C) likely reflect the flexibility, bulk, and nonspherical symmetry of the anions in addition to ionic association strength. (This also explains the differences in the $(G1)_3$:LiX solvate mp's for the same anions.) Vibrational spectroscopy indicates that when the SSIP $(G2)_2$:$LiCF_3SO_3$ solvate melts, most of the ions become CIPs and AGGs.[20,26] In contrast, when the SSIP $(G2)_2$:$LiClO_4$ solvate melts, a large fraction of CIPs form, but a significant fraction of SSIPs remain in the melt and no AGGs are present.[30]

In G3/LiX mixtures, the CIP 1/1 solvates again have mp's reflecting the ionic association ordering:[1]

$$LiCF_3CO_2\ (-48\ °C) < LiNO_3\ (31\ °C) < LiCF_3SO_3\ (40\ °C) < LiBF_4\ (90\ °C) < LiClO_4\ (103\ °C) < LiI\ (119\ °C) < LiAsF_6\ (120\ °C)$$

The crystal structures of the $(G3)_1$:LiX solvates with $LiCF_3SO_3$,[31] $LiBF_4$,[31] $LiClO_4$,[31] and $LiAsF_6$[31] are known. All have the same general structure with each Li^+ cation coordinated by two G3 molecules with four EOs (two from each G3) and a single anion. LiBETI and LiTFSI have been excluded from the comparison since the crystal structure of the CIP $(G3)_1$:LiBETI solvate is quite different (and the $(G3)_1$:LiTFSI solvate structure is unknown).[29] Each Li^+ cation is coordinated by a single G3 molecule with four EOs and a single anion. The differences in these CIP solvates likely reflect the greater bulk of the $BETI^-$ anion which precludes the structure found for the smaller anions.

There is often a considerable hysteresis between the crystallization and melting temperatures of the various glyme−LiX phases.[1] The solvate melts may therefore be supercooled substantially before the nucleation and growth of the crystalline phase. The relative ease with which nucleation of a crystalline

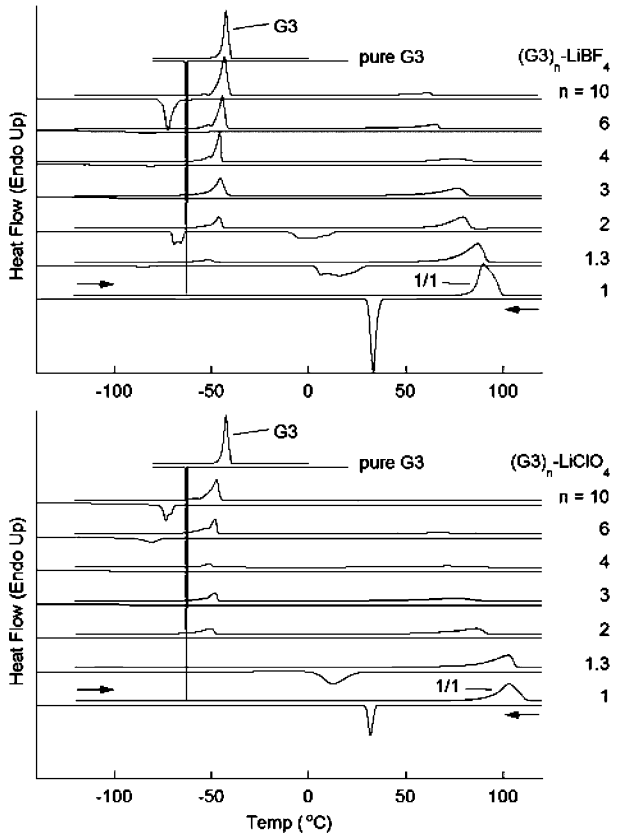

Figure 2. DSC heating and cooling traces of $(G3)_n$−LiX (X = BF_4^-, ClO_4^-) mixtures (10 °C min^{-1}). The plots are normalized to the weight of the G3 in each sample rather than the total sample weight.

Table 1. Comparison of the Crystalline Unit Cell Dimensions for the Isostructural $(G3)_1$:LiX Phases[31]

LiX	*a* (Å)	*b* (Å)	*c* (Å)	*β* (deg)	vol (Å^3)
$LiClO_4$	12.33	6.17	17.29	94.10	1313
$LiBF_4$	12.45	6.22	17.20	93.95	1327
$LiAsF_6$	6.20	12.70	18.54	95.46	1452
$LiCF_3SO_3$	13.02	6.33	18.69	97.28	1528

solvate phase occurs on cooling gives some indication of the nature of the solvates in solution or the melt since the crystal nuclei must reach a critical size before crystal growth occurs. If the amorphous solvates resemble the crystalline solvate, then nucleation is more facile.

$(G3)_n$−LiX Crystallization Kinetics. The CIP 1/1 crystalline solvates, $(G3)_1$:$LiClO_4$ and $(G3)_1$:$LiBF_4$, are isostructural and have similar mp's.[1,31] Further, the unit cells of these crystalline phases are nearly the same since the anions are nearly equivalent in size and shape (Table 1).[31] The ClO_4^- anion has been reported to be ∼10% larger than BF_4^-.[32−38] These similarities in solvate structure make the G3−LiX mixtures ideal for studying the effect of the differences in ionic association strength resulting from different anions on the solvate crystallization kinetics.

Figure 2 shows DSC heating and cooling traces for $(G3)_n$−$LiBF_4$ and $(G3)_n$−$LiClO_4$ mixtures (normalized to the weight fraction of G3 in each sample for ease of comparison). The samples were cooled from room temperature to −120 °C (not shown) after equilibrating several days first at room temperature and then in a freezer. The samples were then heated to 120 °C and cooled to −140 °C (10 °C min^{-1}). The heating scans show the equilibrium behavior of the mixtures, while the cooling scans show the recrystallization behavior of the mixtures from the melt. The crystallization behavior of pure G3 is shown on cooling from room temperature for comparison.

On cooling a $(G3)_n$−$LiBF_4$ (n = 1) mixture, the mixture supercools but then crystallizes fully and relatively easily into the 1/1 phase. The addition of a small excess of G3 hinders the crystallization of the 1/1 phase (n = 1.3 and 2). Once the 1/1 phase has crystallized, however, the remaining G3 is able to crystallize on further cooling. For the n = 3−6 mixtures, the 1/1 phase does not crystallize, and most or all of the G3 also does not crystallize on cooling. These mixtures thus freeze predominantly into amorphous glasses. A significant fraction of the G3 crystallizes in the n = 10 mixture, but the crystallization is significantly hindered relative to the pure G3.

It was difficult to crystallize the dilute $(G3)_n$−$LiClO_4$ (n = 3−10) mixtures (in contrast with the $LiBF_4$ samples). Although the 1/1 phase crystallized readily in a freezer for these mixtures for larger sample sizes (>1 g), this was not the case with the small amounts of the samples (∼10 mg) in the DSC pans. It was difficult or not possible to crystallize the 1/1 phases in these samples. This difference suggests that the difficulty lies in the nucleation of the $(G3)_1$:$LiClO_4$ phase in dilute (n > 2) mixtures. To initiate nucleation in these DSC pans, a small piece of molecular sieve was added to each sample pan. The pans were then stored in a freezer for several days−weeks. The sluggish crystallization is evident in Figure 2 by the smaller amount of G3 which crystallizes in the n = 3−10 samples relative to those with $LiBF_4$. For the $(G3)_n$−$LiClO_4$ (n = 1) mixture, the crystallization of the 1/1 phase is impaired relative to the sample with $LiBF_4$. Less G3 also crystallizes in the dilute samples on cooling.

These results agree with the somewhat higher ionic association of $LiBF_4$ relative to $LiClO_4$ in ether solvents.[1] The dilute G3−LiX mixtures are expected to consist predominantly of an equilibrium between SSIP and CIP solvates:

$$[(EO)_nLi]^+X^- \leftrightarrow [(EO)_mLi^+X^-] + (EO)_{n-m}$$

The equilibrium should be shifted more toward the CIPs on the right for the more associated $LiBF_4$. Some of these CIPs in the melt may resemble the crystalline 1/1 phase facilitating nucleation and crystallization. In contrast, $LiClO_4$ mixtures are expected to contain more SSIPs that those with $LiBF_4$. The Li^+ cations are therefore solvated by more EOs and thus more G3 molecules. This hinders both the crystallization of the CIP 1/1 and G3 crystalline phases.

The solvate phase behavior of glyme−LiI mixtures suggests that LiI may be slightly more dissociated than $LiClO_4$ in ether solvents.[1] The crystal structure of the $(G3)_1$:LiI solvate is not yet known but is expected to resemble that found with $LiBF_4$ and $LiClO_4$. It was not possible to crystallize the CIP 1/1 phase in $(G3)_n$−LiI mixtures with $n \geq 2$.[1] Both the n = 2 and 3 mixtures remained completely amorphous (even after adding a piece of molecular sieve and storing in a freezer for extended periods). Some G3 crystallized in the n = 4−10 samples. In dilute samples, therefore, it is expected that the equilibrium is shifted strongly toward the SSIPs on the left. It may be that relatively stable amorphous SSIP $(G3)_n$−LiI (n = 2) solvates form due to the low ionic association strength of the salt. Even more dissociated salts (i.e., $LiAsF_6$ and LiBETI) apparently stabilize these SSIPs to a greater extent since a 2/1 crystalline phase forms for these latter salts.[1]

$(G4)_n$−LiX Crystallization Kinetics. Figure 3 compares the DSC cooling traces for $(G4)_n$−LiX mixtures (normalized to the weight fraction of G4 in each sample for ease of comparison). It is important to emphasize that these plots show the crystallization of uncoordinated G4. No G4−LiX solvates crystallize for any of the salts for these concentrations.[1] Instead, a fraction

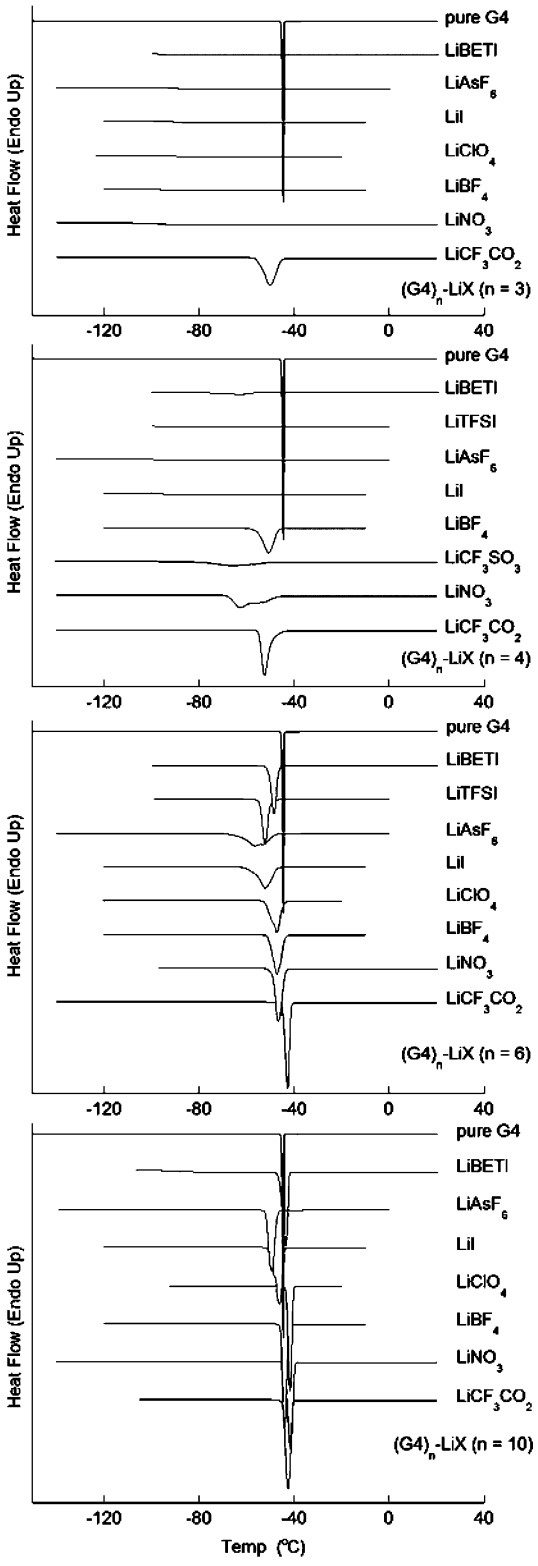

Figure 3. DSC cooling traces of $(G4)_n$−LiX (n = 3, 4, 6, and 10) mixtures (10 °C min^{-1}) showing G4 crystallization exotherms. The plots are normalized to the weight of the G4 in each sample rather than the total sample weight.

of the G4 molecules remain coordinated to the Li^+ cations (with counteranions present) in an amorphous phase. Variations in the ability of the uncoordinated G4 to crystallize can be expected since the degree of interaction of the anions with the cations will influence how many G4 molecules are coordinated to the Li^+ cations and how dispersed these solvates will be. These mixtures therefore permit a study of the fraction of uncoordinated solvent present which is directly linked to the degree of association of the Li^+ cations with the solvent molecules.

Unfortunately, during the course of the investigation of the phase behavior of these mixtures, not all of the sample pans were treated in the same manner. Only the samples that were cooled at the same rate (10 °C min^{-1}) are shown in Figure 3. Some of these samples were cooled initially from room temperature and others from lower temperatures. Those initially cooled from 0 °C or lower had previously been stored in a refrigerator or freezer, respectively, for several days−weeks in hermetically sealed coffee bags. Note that the uncoordinated G4 cannot crystallize at these initial temperatures. Also, no SSIP $(G4)_1$:LiX crystalline solvates form in any of these mixtures (with $n > 1.5$).[1] All of the mixtures are therefore amorphous when the samples were loaded into the DSC instrument, but the samples have not been equilibrated at the same initial temperature which unfortunately detracts somewhat from a direct comparison between the samples. The crystallization behavior of pure G4 is shown on cooling from room temperature for comparison.

On cooling the $(G4)_n$−LiX (n = 3) mixtures, some of the G4 crystallizes only in the sample containing $LiCF_3CO_2$ (i.e., the most associated salt). All of the other mixtures remain amorphous and display a glass transition, T_g, due to the freezing of the solutions into a glassy state. On cooling the $(G4)_n$−LiX (n = 4) mixtures, some G4 crystallization occurs in the mixtures with the more associated salts. The largest fraction and most rapid growth of this phase occurs with $LiCF_3CO_2$. The G4 crystallization is more hindered in the $LiNO_3$ and $LiCF_3SO_3$ mixtures. A significant fraction of G4 also crystallizes in the $LiBF_4$ mixture. The reason for this is unknown but may be due to the storage of this sample in a freezer for several weeks prior to analysis. Interestingly, a small fraction of G4 also crystallizes in the LiBETI mixture. For $(G4)_n$−LiX (n = 6) mixtures, some G4 crystallizes in all of the samples, but the relative ease with which this occurs increases in the order

$$LiAsF_6 < LiI < LiClO_4 < LiBF_4 < LiNO_3 < LiCF_3CO_2$$

Once again, LiBETI (and LiTFSI) appears to be somewhat anomalous in that significant G4 crystallization occurs. The uncoordinated G4 crystallizes relatively easily for the $(G4)_n$−LiX (n = 10) mixtures, although the crystallization is still somewhat sluggish for LiI and $LiAsF_6$.

Although it is possible that three G4 molecules may be able to coordinate a single Li^+ cation (in a manner similar to the SSIP $(G1)_3$:LiX solvates),[39−41] such coordination is improbable due to steric constraints. Thus, most of the Li^+ cations are coordinated by either one or two G4 molecules as amorphous SSIP, CIP, or AGG solvates. With increasing ionic association strength of the LiX salts, the fraction of CIPs and AGGs increases[20,26,42−44] (Figure 4) and less EOs on average will be coordinated to the Li^+ cations. The most associated mixtures, therefore, will have the largest fraction of uncoordinated G4 molecules, in agreement with the crystallization kinetics of G4 observed in Figure 3.

It is interesting that no G4 crystallizes in most of the mixtures with n = 3. This indicates that regions of uncoordinated G4 within the mixtures do not exist in which the nucleation and growth of crystalline G4 may initiate rapidly (under these cooling conditions). Only with $LiCF_3CO_2$ do such regions exist, but the broad exothermic peak indicates that the growth of the crystalline G4 phase is still sluggish. G4 crystallization is also inhibited in the n = 4 samples with LiI and more dissociated salts.

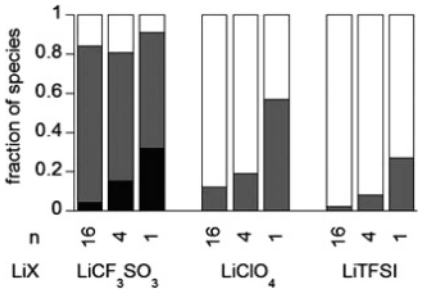

Figure 4. Fractions of solvate species determined from literature vibrational spectroscopic studies of ionic association in $(G4)_n$−LiX (n = 1, 4, and 16) mixtures at 25 °C (black: AGGs; gray: CIPs; white: "free" anions/SSIPs).[20,26,36−38]

P(EO)$_n$−LiX Crystallization Kinetics. The crystallization behavior of P(EO)$_n$−LiX mixtures has been studied with low molecular weight PEO(2000) (below the PEO entanglement limit of 3200).[45] The same crystalline phases form with the low and high molecular weight PEO at room temperature. This was verified by the author using powder XRD (not shown). Mixtures with $n = 3-14$ were examined with different salts (note that n is now the EO/Li ratio rather than the glyme/Li ratio). The fully crystalline mixtures were initially heated (10 °C min^{-1}) to ∼ 20 °C above the mp of the highest melting phase. The mixtures were then quenched (320 °C min^{-1}) to −100 °C and heated again (10 °C min^{-1}) (Figures 5 and 6). To complement this study, P(EO)$_n$(2000)−LiX and P(EO)$_n$(5×10^6)−LiX mixtures were also sealed in glass capillary tubes, heated to the melt state, and then rapidly cooled to room temperature. The powder XRD patterns of the samples were then followed as a function of time to examine the rates of crystallization at room temperature (Figure 7). Some speculation is given below for the observed differences in crystallization of the phases.

For the P(EO)$_n$−$LiAsF_6$ and −$LiPF_6$ mixtures, SSIP 6/1 crystalline phases are known for both salts,[46−48] and an AGG 3/1 crystalline phase has been reported for $LiAsF_6$.[49] The SSIP 6/1 phase crystallizes very rapidly (much of it during the quenching step for $LiAsF_6$) for the $n = 6$ sample (Figure 5). With excess EOs (i.e., $n > 6$), crystallization of the SSIP 6/1 phase is slower but still relatively fast. Note that the SSIP 6/1 phase crystallizes before the excess PEO in the $n = 8$ and 10 samples, suggesting that the salt is dispersed (hindering PEO crystallization) until the SSIP 6/1 phase forms. A small amount of excess PEO is able to crystallize on heating the $n = 14$ sample. It was difficult to form homogeneous samples for concentrations of $n < 6$ due to the thermal instability of the mixtures. The small endothermic peak for the $LiPF_6$ sample with $n = 3$ may thus be due to some SSIP 6/1 phase present. (This sample decomposed above about 120 °C.) For the most dissociated salts such as these, although the local Li^+ cation coordination may remain much the same in the melt, the manner of coordination (one polymer chain or two) may change. To interpret these results, recall that at room temperature the SSIP 6/1 phase with both salts consist of Li^+ cations coordinated by two PEO chains with uncoordinated anions located between the resulting polymer−cation cylinders.[47,48] A novel high-temperature SSIP 6/1 phase for $LiAsF_6$ has also recently been reported in which the Li^+ cations are instead coordinated by a single PEO chain.[50] Such a phase transition had been previously noted for the SSIP 6/1 phase of P(EO)$_n$(2000)−$LiSbF_6$ ($n = 6$).[51] At low temperature, the cooperative coordination of the Li^+ cations by two polymer chains may be highly favorable, but at high temperature the molecular motion of the polymer chains is likely to hinder the alignment of two chains about a row of cations.

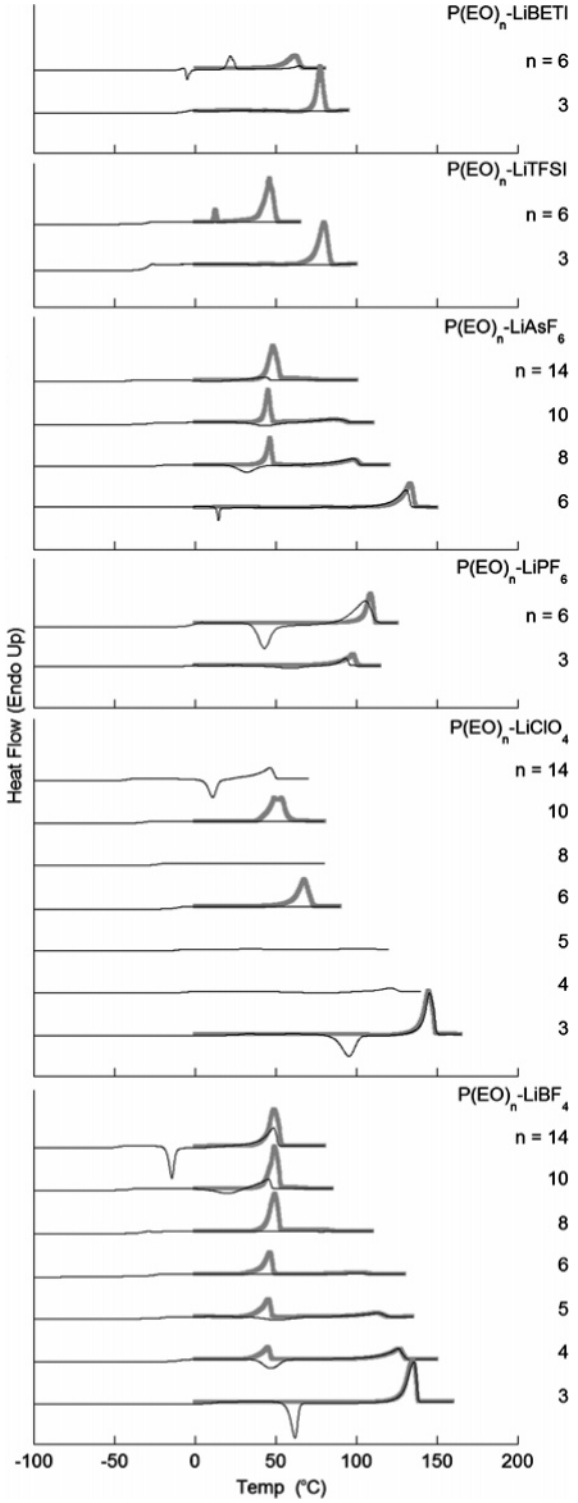

Figure 5. DSC heating traces of P(EO)$_n$(2000)−LiX mixtures (thick gray line: first heating at 10 °C min^{-1}, the samples were then quenched to −100 °C at 320 °C min^{-1}; thin black line: second heating at 10 °C min^{-1}).

Therefore, single-chain coordination of the Li^+ cations predominates (still as SSIPs for the highly disassociated salts) at higher temperatures in agreement with spectroscopic characterization,[51] resulting in the new crystalline phase. The crystallization of this single-chain SSIP 6/1 phase accounts for the rapid crystallization as the samples are cooled and/or reheated.

For the P(EO)$_n$−LiBETI and −LiTFSI mixtures, the samples with $n = 8-10$ were viscous liquids that did not crystallize fully even after storage in a freezer for 2 months. Some of the

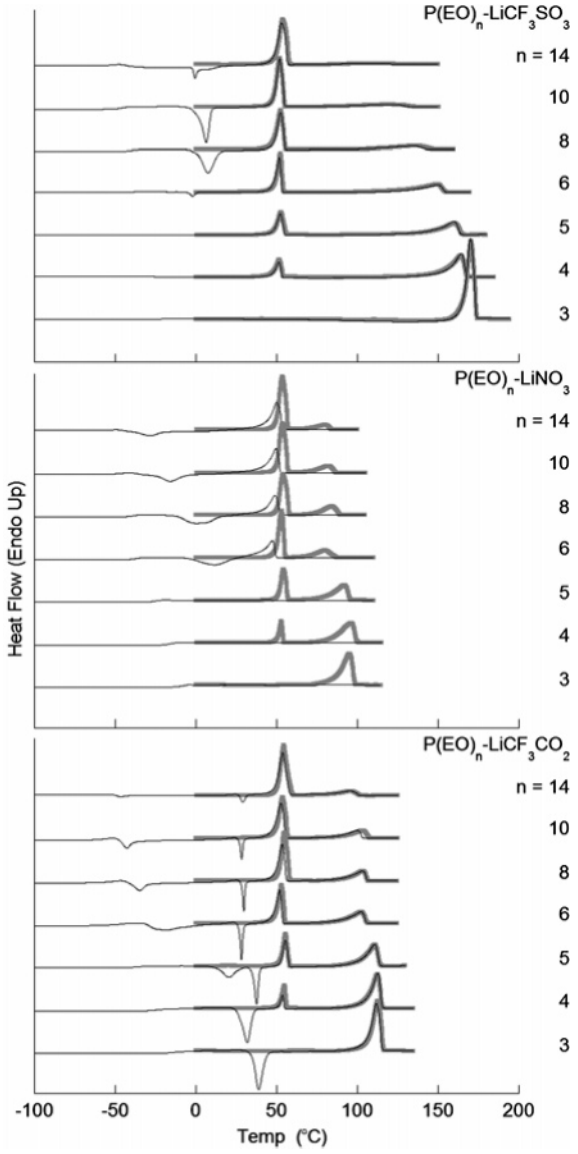

Figure 6. DSC heating traces of $P(EO)_n(2000)-LiX$ mixtures (thick gray line: first heating at 10 °C min^{-1}, the samples were then quenched to −100 °C at 320 °C min^{-1}; thin black line: second heating at 10 °C min^{-1}).

PEO in the $n = 10$ and 14 samples crystallized slowly (a white solid formed in the liquids). Note that a small amount of PEO crystallizes in the high-MW PEO samples with LiTFSI and LiBETI (Figures 1 and 7). It was difficult to get homogeneous $n = 3-6$ samples. These salts are known to form SSIP 6/1 and AGG 3/1 crystalline phases.[5,49,52−54] Note that both the SSIP 6/1 and AGG 3/1 phases are slow to crystallize with both LiBETI and LiTFSI (Figures 1, 5, and 7). The very slow crystallization kinetics of $P(EO)_n-LiTFSI$ mixtures ($n > 7$) for the SSIP 6/1 phase has been denoted as a "crystallinity gap".[5,9,52] The origin of the crystallinity gap remains unknown, but note that, even in the melt state, the Li^+ cations in $P(EO)_n-LiTFSI$ mixtures ($n > 7$) exist almost entirely (>90%) as SSIP solvates.[55] In contrast, in the melt state, a significant fraction (~25%) of CIP solvates form in an $n = 6$ mixture.[55] Thus, an amorphous phase forms in the melt when excess EOs are present with an EO/Li concentration of ~8−9 and the Li^+ cations fully solvated by the EOs as SSIPs. This phase is nearly as thermodynamically favorable as the SSIP 6/1 crystalline phase. One possibility is that the 6/1 crystalline phase has the Li^+ cations coordinated to two PEO chains, but once melted most of the Li^+ cations are coordinated by a single chain. A new crystalline SSIP 6/1 phase does not form (as with $LiAsF_6$ and $LiSbF_6$) because the bulky $TFSI^-$ anions cannot pack together in the same manner as do the smaller anions. Thus, "spacers" of 2−3 uncoordinated EOs separate the Li^+ cations coordinated to 6 EOs on a single chain. These spacers and the disorder they introduce hinder crystallization. This argument is purely speculative. The origin of the lower temperature endothermic peaks for both salts is unclear and is the topic of a separate study.

For the $P(EO)_n-LiClO_4$ mixtures, SSIP 6/1 and AGG 3/1 phases are known.[11,46,56] Quenching the $n = 3$ sample from the melt forms a glass, but crystallization of the AGG 3/1 phase occurs readily on heating (Figure 5). Excess EOs ($n = 4$ and 5) hinder the crystallization of the AGG 3/1 phase—some of the AGG 3/1 phase recrystallized in the $n = 4$ sample, but the $n = 5$ sample remained amorphous. No recrystallization of the 6/1 phase occurred on heating the $n = 4$ and 5 samples. The $n = 6-10$ samples remained amorphous during the second heating step, but a relatively large fraction of the excess PEO in the $n = 14$ sample was able to recrystallize. In general, it was difficult to form homogeneous, fully crystallized samples with this salt and PEO(2000). The recrystallization of the SSIP 6/1 phase with $PEO(5 \times 10^6)$ is slow[11] (requiring days; Figure 7) and extremely slow with PEO(2000) (requiring months to partially crystallize into the SSIP 6/1 phase). The very slow recrystallization kinetics with $LiClO_4$ appear to be due to the formation of very stable amorphous CIP solvates[56] which hinder the crystallization of both the AGG 3/1 and SSIP 6/1 phases.

For the $P(EO)_n-LiBF_4$ mixtures, no SSIP 6/1 phase forms (Figure 5). The AGG 3/1 phase[27] was able to fully recrystallize in the $n = 3$ sample during the second heating step (Figure 5). For more dilute samples ($n = 4-8$), the excess PEO remains amorphous during the second heating step, but the 3/1 phase crystallizes. Some of the excess PEO was able to recrystallize for the more dilute ($n = 10$ and 14) samples. The salt dissolved in the amorphous phase hinders the crystallization of the PEO phase, even for the $n = 8$ concentration. At room temperature, the recrystallization of the 3/1 phase in $n = 6$ and 10 samples requires minutes to hours (Figure 7).

For the $P(EO)_n-LiCF_3SO_3$ mixtures, no SSIP 6/1 phase forms (Figure 6).[5,46] The AGG 3/1[57] and excess PEO phases were able to recrystallize very rapidly (during quenching) for the $n = 3-5$ samples. A small fraction of the sample remained amorphous until the second heating step for the $n = 6$ sample. The amount of amorphous fraction increases for the more dilute samples ($n > 6$), but both the AGG 3/1 and PEO phases completely crystallized during the second heating step. Vibrational spectroscopy has shown that in the melt state most of the anions in a $P(EO)_n-LiCF_3SO_3$ ($n = 3$) mixture retain the same $Li^+...CF_3SO_3^-...Li^+$ AGG form of coordination found in the AGG 3/1 crystal structure in which two of the anion oxygens coordinate two cations.[58] The amorphous solvates in the melt thus resemble the crystalline phase, and nucleation is facile. In more dilute mixtures, however, a greater fraction of CIPs and SSIPs form in the melt (an exception to the observation of increasing ionic association with increasing temperature)[7] which hinders the crystallization of the AGG 3/1 phase somewhat (as seen by the melts with $n \geq 8$ which remain amorphous during the quenching step and crystallize instead during the second heating step).

For the $P(EO)_n-LiNO_3$ mixtures, no SSIP 6/1 phase forms (Figure 6). The AGG 3/1 phase does not recrystallize easily in any of the samples. The $n = 3-5$ samples remain amorphous on the second heating step while some of the excess PEO is

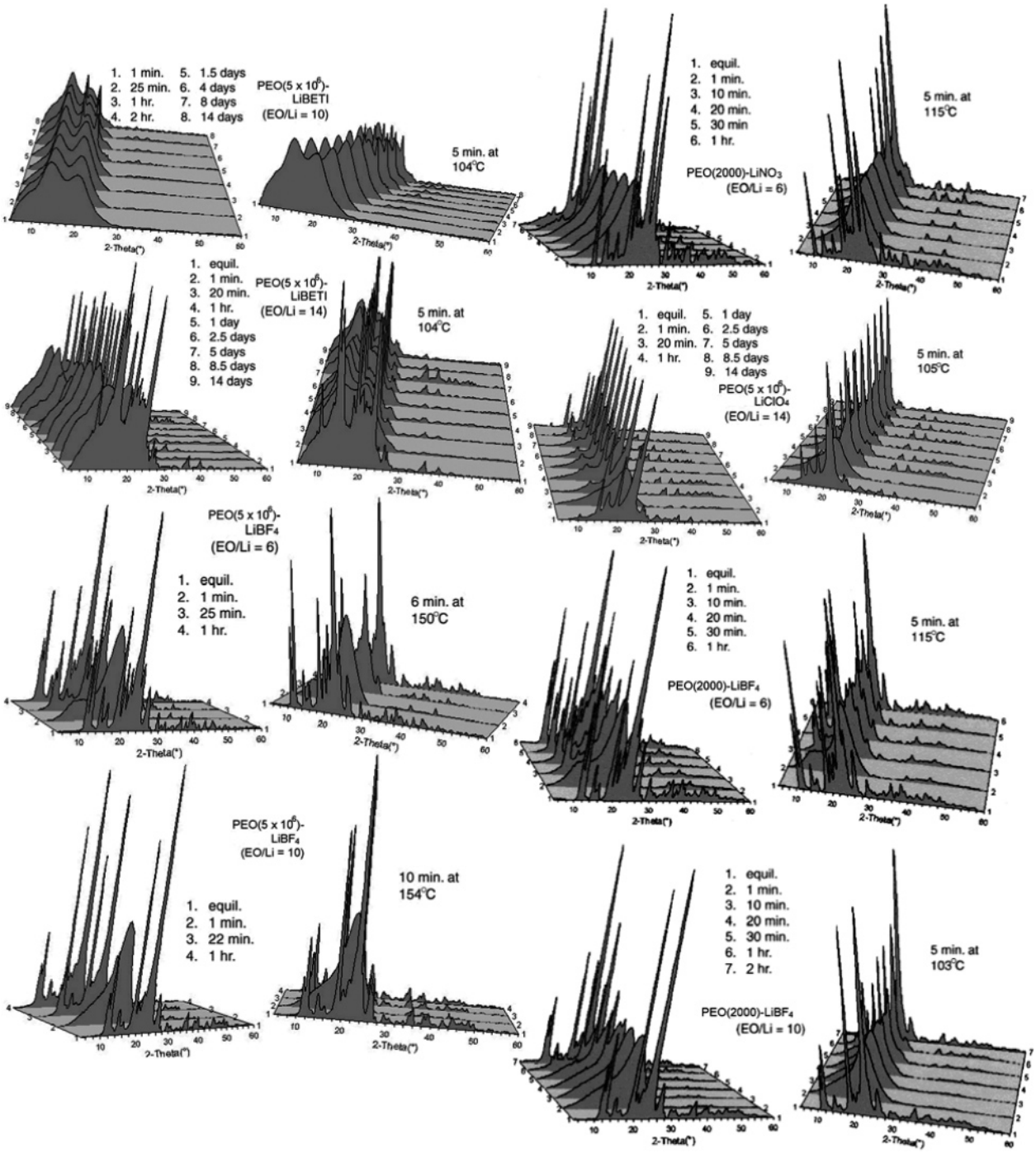

Figure 7. Powder XRD plots at 25 °C shown for different times after quenching from the melt at the indicated temperature (equilibrium indicates the initial fully crystalline electrolyte—two views shown for each sample). Melting temperature and time indicated.

able to crystallize for more dilute ($n > 6$) samples (Figures 6 and 7). $LiNO_3$ was found to salt-out of very concentrated G4−$LiNO_3$ mixtures and when heating G1−$LiNO_3$ mixtures.[1] It may be that heating the concentrated samples with PEO to form a melt causes the salt to form aggregates which differ from those found in the AGG 3/1 phase and may resemble crystalline $LiNO_3$ (note the two small diffraction peaks present in Figure 7 at higher 2θ values when the $P(EO)_n(2000)-LiNO_3$ ($n = 6$) sample is amorphous).[59] These AGGs hinder the crystallization of the AGG 3/1 phase but permit some of the PEO to crystallize.

For the $P(EO)_n-LiCF_3CO_2$ mixtures, no SSIP 6/1 phase forms (Figure 6). The AGG 3/1 and excess PEO phases were able to recrystallize on the second heating step for all of the samples similar to the samples with $LiCF_3SO_3$. But for the most concentrated samples, the mixtures remained amorphous on quenching and only crystallize during the second heating step. For the most dilute samples, some of the excess PEO recrystallizes during the quenching step. The AGG 3/1 phase is likely to consist of $CF_3CO_2^-$ anions coordinated to two Li^+ cations. The $(G2)_{1/3}$:$LiCF_3CO_2$ and $(G4)_{2/5}$:$LiCF_3CO_2$ crystalline solvate structures, however, have some anions which are also coordinated to three or even four Li^+ cations.[31,60] This salt is more associated than $LiCF_3SO_3$ so it may be that in the melt AGG solvates form in which the anions become coordinated to more than two Li^+ cations. These different forms of AGG solvates may slightly hinder the recrystallization of the AGG 3/1 phase. The excess PEO does not appear to participate in the cation solvation as reflected in the ease of the PEO crystallization.

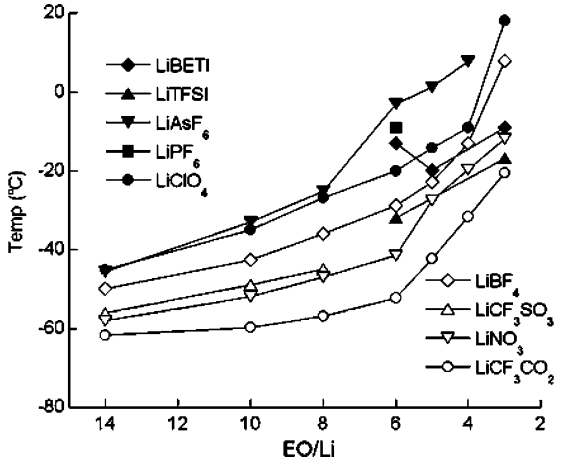

Figure 8. Glass transition temperatures (T_g) (from data in Figures 5 and 6) vs EO/Li concentration for P(EO)$_n$(2000)−LiX mixtures.

Note that the NO_3^- anion may not be able to form such complex aggregates. Thus, $LiNO_3$ instead salts-out (crystallizes).[59]

Glass Transition (T_g) of P(EO)$_n$(2000)−LiX Mixtures. Figure 8 shows a plot of the T_g values for the P(EO)$_n$(2000)−LiX mixtures from the data in Figures 5 and 6 (second heating after quenching). Data are only shown for the samples that remained amorphous during the quenching step. It is clear that the general trend is for the T_g values to increase with higher salt concentration and more dissociated salts:

$$LiCF_3CO_2 < LiNO_3 < LiCF_3SO_3 < LiBF_4 < LiClO_4 < LiAsF_6$$

This agrees with the expectation that the most dissociated salts (those in which the cations interact with the anions most weakly) will be solvated by the most EOs from one or more polymer chains. LiTFSI (and perhaps LiBETI) alone do not agree with this trend (from the limited data presented). The reason for this is not known but may be due to the large size and flexibility of the anions which influences the local Li^+ cation solvation. Note that two T_gs are clearly present for the $n = 10$ and 14 samples with $LiCF_3CO_2$. This salt is the most associated of the salts studied. The Li^+ cations are likely to be solvated by single PEO chains and multiple anions forming aggregate clusters. Thus, even in the amorphous melt, the salt may concentrate into salt-rich and salt-poor regions, resulting in separate T_gs as observed in poly(propylene oxide) electrolytes.[61]

4. Conclusion

The crystallization kinetics for glyme−LiX and PEO−LiX mixtures have been examined. Wide variations in the crystallization of the phases are noted which are salt-dependent. These differences have been well correlated with the relative ionic association strength of the salts in aprotic solvents. For moderately concentrated (EO/Li > 6) electrolytes in the melt, the Li^+ cation solvates tend to remain uncoordinated by the anions for the most dissociating of the salts (e.g., $LiAsF_6$), whereas more highly associating salts (e.g., $LiNO_3$ and $LiCF_3CO_2$) will form even more aggregated solvates or the lithium salt may salt-out of the mixture. For more dilute electrolytes in the melt, association can actually decrease as the salt is dispersed in the polyether solvent, even for relatively highly associating salts (e.g., $LiCF_3SO_3$), but aggregation of the solvates occurs as the temperature is reduced and thermal disorder decreases. Scrutiny of the crystallization kinetics, in addition to examining the phase behavior and crystal structures of solvates, is shown to be yet another informative methodology for understanding the properties of liquid and amorphous solid electrolytes.

Acknowledgment. W.A.H. is indebted to the National Science Foundation for the award of a NSF Graduate Research Fellowship and the University of Minnesota for a Graduate Research Fellowship.

References and Notes

(1) Henderson, W. A. *J. Phys. Chem. B* **2006**, *110*, 13177.
(2) Ferloni, P.; Chiodelli, G.; Magistris, A.; Sanesi, M. *Solid State Ionics* **1986**, *18−19*, 265.
(3) Neat, R.; Glasse, M.; Linford, R.; Hooper, A. *Solid State Ionics* **1986**, *18−19*, 1088.
(4) Yang, L.; Zhang, A.; Qiu, B.; Yin, J.; Liu, Q. *Solid State Ionics* **1988**, *28−30*, 1029.
(5) Vallée, A.; Besner, S.; Prud'homme, J. *Electrochim. Acta* **1992**, *37*, 1579.
(6) Gray, F. M. *Solid Polymer Electrolytes—Fundamentals and Technological Applications*; VCH Publishers: New York, 1991; pp 74−78.
(7) Chintapalli, S.; Frech, R. *Electrochim. Acta* **1998**, *43*, 1395.
(8) Frech, R.; Chintapalli, S.; Bruce, P. G.; Vincent, C. A. *Macromolecules* **1999**, *32*, 808.
(9) Edman, L.; Ferry, A.; Doeff, M. M. *J. Mater. Res.* **2000**, *15*, 1950.
(10) Dygas, J. R.; Misztal-Faraj, B.; Florjańczyk, Z.; Krok, F.; Marzantowicz, M.; Zygad[swsl]lo-Monikowska, E. *Solid State Ionics* **2003**, *157*, 249.
(11) Henderson, W. A.; Passerini, S. *Electrochem. Commun.* **2003**, *5*, 575.
(12) Choi, B. K.; Kim, Y. W. *Mater. Sci. Eng.* **2004**, *B107*, 244.
(13) Choi, B.-K.; Kim, Y.-W. *Electrochim. Acta* **2004**, *49*, 2307.
(14) Choi, B.-K. *Solid State Ionics* **2004**, *168*, 123.
(15) Volel, M.; Armand, M.; Gorecki, W. *Macromolecules* **2004**, *37*, 8373.
(16) Marzantowicz, M.; Dygas, J. R.; Jenninger, W.; Alig, I. *Solid State Ionics* **2005**, *176*, 2115.
(17) Marzantowicz, M.; Dygas, J. R.; Krok, F.; Lasińska, A.; Florjańczyk, Z.; Zygadlo-Monikowska, E.; Affek, A. *Electrochim. Acta* **2005**, *50*, 3969.
(18) Marzantowicz, M.; Dygas, J. R.; Krok, F.; Zygadlo-Monikowska, E.; Florjanczyk, Z. *Mater. Sci.* **2006**, *24*, 195.
(19) Marzantowicz, M.; Dygas, J. R.; Krok, F.; Lasinska, A.; Florjanczyk, Z.; Zygadlo-Monikowska, E. *Electrochim. Acta* **2006**, *51*, 1713.
(20) Huang, W. Ph.D. Thesis, The University of Oklahoma, 1994.
(21) Becker, G.; Eschbach, B.; Mundt, O.; Reti, M.; Niecke, E.; Issberner, K.; Nieger, M.; Thelen, V.; Nöth, H.; Waldhör, R.; Schmidt, M. *Z. Anorg. Allg. Chem.* **1998**, *624*, 469.
(22) Rogers, R. D.; Bynum, R. V.; Atwood, J. L. *J. Crystallogr. Spectrosc. Res.* **1984**, *14*, 29.
(23) Ramírez, A.; Lobkovsky, E.; Collum, D. B. *J. Am. Chem. Soc.* **2003**, *125*, 15376.
(24) Henderson, W. A.; Brooks, N. R.; Brennessel, W. W.; Young, Jr., V. G. *J. Phys. Chem. A* **2004**, *108*, 225.
(25) Riffel, H.; Neumüller, B.; Fluck, E. *Z. Anorg. Allg. Chem.* **1993**, *619*, 1682.
(26) Frech, R.; Huang, W. *Solid State Ionics* **1994**, *72*, 103.
(27) Andreev, Y. G.; Seneviratne, V.; Khan, M.; Henderson, W. A.; Frech, R. E.; Bruce, P. G. *Chem. Mater.* **2005**, *17*, 767.
(28) Seneviratne, V.; Frech, R.; Furneaux, J. E.; Khan, M. *J. Phys. Chem. B* **2004**, *108*, 8124.
(29) Henderson, W. A.; McKenna, F.; Khan, M. A.; Brooks, N. R.; Young, Jr., V. G.; Frech, R. *Chem. Mater.* **2005**, *17*, 2284.
(30) Grondin, J.; Ducasse, L.; Bruneel, J.-L.; Servant, L.; Lassègues, J.-C. *Solid State Ionics* **2004**, *6*, 441.
(31) Henderson, W. A.; Brooks, N. R.; Brennessel, W. W.; Young, Jr., V. G. *Chem. Mater.* **2003**, *15*, 4679.
(32) Ue, M. *J. Electrochem. Soc.* **1994**, *141*, 3336.
(33) Van Rensburg, D. J. J.; Boeyens, J. C. A. *J. Solid State Chem.* **1972**, *5*, 79.
(34) Prask, H. J.; Choi, C. S.; Chesser, N. J.; Rosasco, G. J. *J. Chem. Phys.* **1988**, *88*, 5106.
(35) Palacios, E.; Melero, J. J.; Burriel, R.; Ferloni, P. *Phys. Rev. B* **1996**, *54*, 9099.
(36) Palacios, E.; Burriel, R.; Ferloni, P. *Acta Crystallogr.* **2003**, *B59*, 625.
(37) Giuseppetti, G.; Tadini, C.; Ferloni, P.; Zabinska, G.; Torre, S. *Z. Kristallogr.* **1994**, *209*, 509.
(38) Kivikoski, J.; Howard, J. A. K.; Kelly, P.; Parker, D. *Acta Crystallogr.* **1995**, *C51*, 535.
(39) Näther, C.; Bock, H. *Acta Crystallogr.* **1995**, *C51*, 2510.
(40) Schumann, H.; Nickel, S.; Loebel, J.; Pickardt, J. *Organometallics* **1988**, *7*, 2004.

(41) Näther, C.; Bock, H.; Havlas, Z.; Hauck, T. *Organometallics* **1998**, *17*, 4707.
(42) Grondin, J.; Lassègues, J.-C.; Chami, M.; Servant, L.; Talaga, D.; Henderson, W. A. *Phys. Chem. Chem. Phys.* **2004**, *6*, 4260.
(43) Firman, P.; Xu, M.; Eyring, E. M.; Petrucci, S. *J. Phys. Chem.* **1993**, *97*, 3606.
(44) Brouillette, D.; Irish, D. E.; Taylor, N. J.; Perron, G.; Odziemkowski, M.; Desnoyers, J. E. *Phys. Chem. Chem. Phys.* **2002**, *4*, 6063.
(45) Shi, J.; Vincent, C. A. *Solid State Ionics* **1993**, *60*, 11.
(46) Robitaille, C. D.; Fauteux, D. *J. Electrochem. Soc.* **1986**, *133*, 315.
(47) MacGlashan, G. S.; Andreev, Y. G.; Bruce, P. G. *Nature (London)* **1999**, *398*, 792.
(48) Gadjourova, Z.; y Marero, D. M.; Andersen, K. H.; Andreev, Y. G.; Bruce, P. G. *Chem. Mater.* **2001**, *13*, 1282.
(49) Martin-Litas, I.; Andreev, Y. G.; Bruce, P. G. *Chem. Mater.* **2002**, *14*, 2166.
(50) Staunton, E.; Andreev, Y. G.; Bruce, P. G. *J. Am. Chem. Soc.* **2005**, *127*, 12176.
(51) Seneviratne, V.; Frech, R.; Furneaux, J. E. *Electrochim. Acta* **2003**, *48*, 2221.
(52) Lauscaud, S.; Perrier, M.; Vallée, A.; Besner, S.; Prud'homme, J.; Armand, M. *Macromolecules* **1994**, *27*, 7469.
(53) Andreev, Y. G.; Lightfoot, P.; Bruce, P. G. *Chem. Commun.* **1996**, 2169.
(54) Appetecchi, G. B.; Henderson, W.; Villano, P.; Berrettoni, M.; Passerini, S. *J. Electrochem. Soc.* **2001**, *148*, A1171.
(55) Edman, L. *J. Phys. Chem. B* **2000**, *104*, 7254.
(56) Ducasse, L.; Dussauze, M.; Grondin, J.; Lassègues, J.-C.; Naudin, C.; Servant, L. *Phys. Chem. Chem. Phys.* **2003**, *5*, 567.
(57) Lightfoot, P.; Mehta, M. A.; Bruce, P. G. *Science* **1993**, *262*, 883.
(58) Frech, R.; Chintapalli, S.; Bruce, P. G.; Vincent, C. A. *Chem. Commun.* **1997**, 157.
(59) Wu, X.; Fronczek, F. R.; Butler, L. G. *Inorg. Chem.* **1994**, *33*, 1363.
(60) Henderson, W. A.; Young, Jr., V. G.; Brooks, N. R.; Smyrl, W. H. *Acta Crystallogr.* **2002**, *C58*, m501.
(61) Bégin, M.; Vachon, C.; Labrèche, C.; Goulet, B.; Prud'homme, J. *Macromolecules* **1998**, *31*, 96.

MA061866D